Heat to H$_2$

Using Waste Heat to Set Up Concentration Differences for Reverse Electrodialysis Hydrogen Production

Ellen S. Skilbred*[a], Kjersti W. Krakhella*[a], Ida J. Haga*[a], Jon G. Pharoah[b], Magne Hillestad[c], Gonzalo d. A. Serrano[d] and Odne S. Burheim[a]

*Shared first authorship
[a]Dep. of Energy and Process Engineering, NTNU, Norway

[b]Dep. of Mechanical and Materials Engineering, Queen's University, Canada
[c]Dep. of Chemical Engineering, NTNU, Norway

[d]SINTEF Energy Research AS, Norway

Abstract

The present work suggests two concepts for producing hydrogen by reverse electrodialysis. Reverse electrodialysis is a technology that uses concentration differences to create electrical energy. In this work, the energy is utilised as direct hydrogen production within a closed-loop system. For both system alternatives, waste heat is used to set up the mentioned concentration differences. The first concept is evaporation, where heat is added to boil off excess water from a concentrated solution and thereby increase its concentration. The second concept removes heat to precipitate excess salt. For the precipitation concept to work, a salt where the solubility is highly dependent on temperature must be used. KNO$_3$ fulfils this requirement. As part of a proof of concept, the conductivity of membranes soaked in KNO$_3$ was investigated. The conductivity of the salt in two commercialised membranes, Fumatech FKE-50 and FAS-30, was measured and compared to NaCl in the same membranes. The conductivity of K$^+$ in FKE-50 was found to be 4.5 and 6.6 mS cm^{-1} at 25 °C and 40 °C respectively. The conductivity of NO$_3^-$ in FAS-30 was found to be 4.3 mS cm^{-1} and 6.5 mS cm^{-1} at 25 °C and 40 °C respectively. Neither of the membranes change conductivity with soaking concentrations. The conductivity at 40 °C compared to 25 °C is significantly better in the FKE membrane, and seemingly better in the FAS membrane. Potential peak power densities for a

RED unit cell is 2.31 W m^{-2} with the precipitation system, and 108 W m^{-2} when evaporation is used.

Introduction

The increased global energy demand and undesired climate changes motivates studies of new renewable energy sources. Energy for the future needs to be rapidly provided, dependable and have as low negative impact as possible. The most commercial renewable energy technologies, like wind and photovoltaics, delivers energy intermittently and electrically. Supply and consumption fluctuations do not necessarily match, making energy storage important to provide energy where and when it is needed. Storing renewable energy in hydrogen is one alternative to handle the potential mismatch of energy supply and consumption. This article suggests two methods for converting waste heat to hydrogen through reverse electrodialysis (RED).

RED is a technology that converts the energy of mixing two solutions of different salinity to electrical energy while driving a red-ox reaction (19, 23). Ionic solutions of different concentrations are supplied on each side of an ion exchange membrane. Ions will then seek to even out concentration differences and travel through the membrane. This, in turn, establishes an electrical potential, which increases when several membranes are combined in a stack. When the potential established by the reverse electrodialysis is higher than the potential required for water splitting, hydrogen evolution is possible (12, 20). Anion and cation exchange membranes (AEM and CEM) control the transport of ions from the concentrated to the dilute solutions. A RED stack is illustrated in Fig. 1.
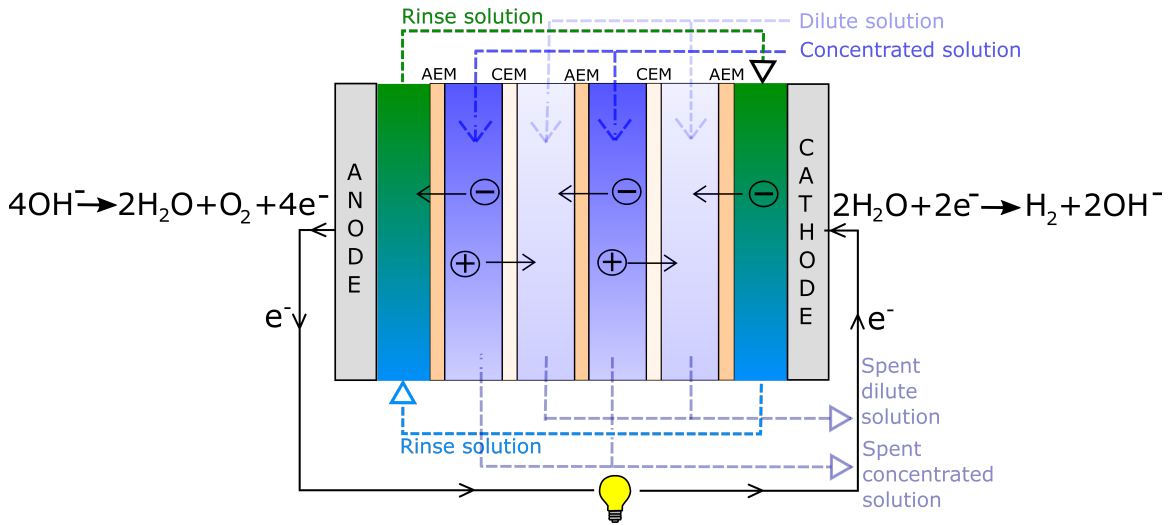

Figure 1. Illustration of a RED-cell. Hydrogen is produced by the cathode and oxygen at the anode.

The open circuit potential, E_{ocp} [V], over a RED unit cell is given by

$$E_{ocp} = \alpha \frac{RT}{zF} \ln \left(\frac{a_c}{a_d} \right)$$

[1]

where α is the permselectivity of the membrane, R is the gas constant, T [K] is the temperature, z is the valence number of the ion transported, F is Faraday's constant, and a is the activity of the transported ion in the concentrated, c, and dilute, d, solutions (2).

The total potential in a unit cell is given in Eq. 2. Non-ohmic losses are not considered in this paper.

$$E = E_{\text{ocp}} - rj \qquad [2]$$

where j is the current density in A m^{-2}. Area resistance r [Ω m^2] is given in Eq. [3].

$$r = r_{\text{d}} + r_{\text{c}} + r_{\text{CEM}} + r_{\text{AEM}} \qquad [3]$$

The resistance of the solutions, r_{d} and r_{c} is the solution resistivity, ρ [Ω m], multiplied with the compartment thickness, and r_{CEM} and r_{AEM} are the resistance of the membranes. The power density is the cell potential multiplied with the current density.

$$P = E_{\text{ocp}}j - rj^2 \qquad [4]$$

The first focus of RED was to exploit the energy of mixing when natural seawater mix with less saline water (13, 19, 22, 23). In the later years, attention has been given to closed-loop RED stacks, where heat is utilised for reversing the salt solutions back to their original concentrations (10, 14, 15, 17, 24). The recycling of solutions increase the economical feasibility of using other salts than NaCl and allows for a freer choice of concentrations than those found in nature, in addition to preventing fouling mechanisms. From Eq. [1] we see that it is beneficial with a large concentration gradient over the membrane and a high temperature. The latter was tested experimentally by Długołęcki et al. and Van Egmond et al. (3, 21), among others.

The cell potential will be lower than the theoretical for a number of reasons, including concentration polarisation and ohmic losses. When compartment thicknesses and solution concentrations are optimised, ionic resistance in the membranes is the main contributor to ohmic losses (9, 13).

We suggest reversing the concentrations used in RED by either evaporating water from the used concentrate or precipitating a slurry from the used dilute. An ideal salt solution would have a pronounced change in its solubility in response to temperature changes. NaCl, which is the salt most used in RED experiments, do not have a steep solubility curve slope, and will thus not give significant potential in the precipitation system. An alternative is KNO$_3$, where a higher potential is achievable given that membrane conductivity is not a limiting factor. To investigate this, conductivity measurements of AEMs and CEMs soaked in KNO$_3$ at 25 °C and 40 °C are performed for concentrations up to the saturation point

Concept

The phase separation process is the key to regenerate spent solutions in the closed-loop RED-systems that are presented. If the spent electrolytes are recovered, heat may be used to restore them to their initial states. This ensures that heat is the only consumable in the system, preferably at as low temperature as possible. Such heat is of low quality and is seldom put to use, often referred to as low grade waste heat (4). As mentioned, two methods for separation are presented; evaporation and precipitation.

As the achievable concentration difference will differ between the techniques, the stack potential is likely to differ too. Simultaneously, the heat and temperatures required to run the process are not the same in the two cases and this may affect the internal energy consumption. This will be elaborated in the next two sections.

Evaporation

A principle sketch of a separation system using evaporation is shown in Fig. 2a. Here, external heat is added to the concentrate, making the water boil off at low pressure. Eventually, the concentration will be high enough for the original potential to be restored, while the removed water will ensure a low concentration in the dilute electrolyte. For improved energy efficiency, the condensation energy of the pure water should be used to maintain the temperature in the separation container.
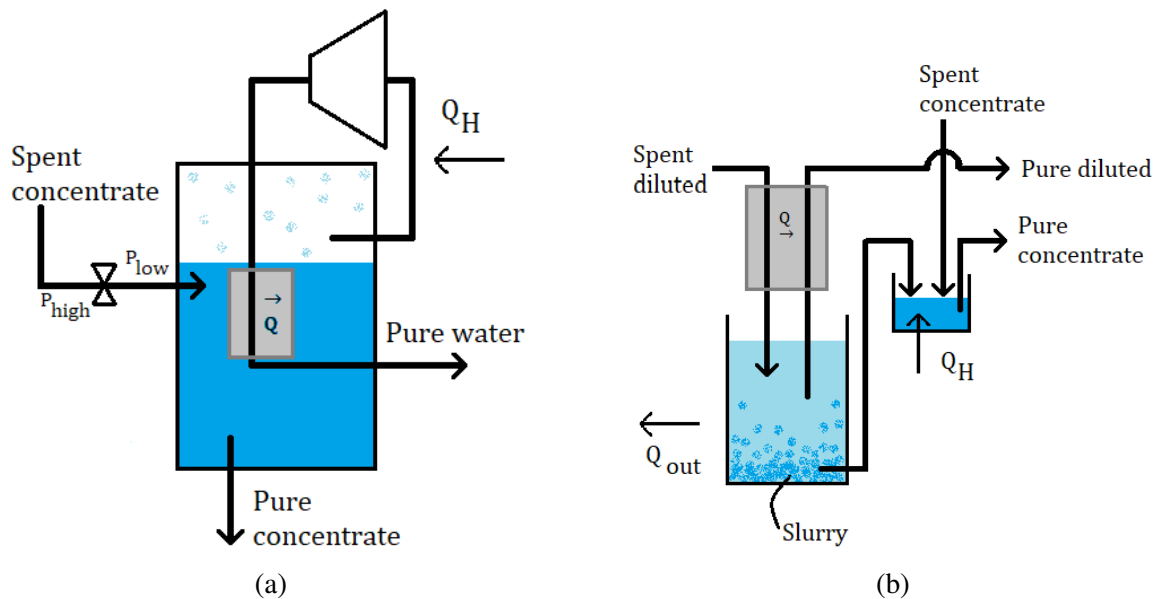

Figure 2. Sketch of principle of (a) separation by evaporation and (b) separation by precipitation

This separation system is presumably energetically disadvantageous, as large quantities of heat are required to make the water evaporate and because of the need for compressor power. Heat exchange capacity is also associated with large capital costs. However,

this system allows for lower concentrations in the dilute compartment, as the precipitation temperature is no longer a limitation. This increases the possible Nernst potential. This electrical gain must be weighted against the disadvantages when the system is evaluated. If the heat added is surplus, meaning that it would not have been put to any other use, the actual heat quantity and temperature may be of less importance.

Precipitation

As previously mentioned, the salt used in this concept needs to have solubility that change substantially with temperature. The dilute concentration in the RED stack is at the solubility limit at a low temperature while the concentrated concentration equals the saturation concentration at a higher temperature. The stack will be operated under conditions where neither solution will spontaneously precipitate, ensuring that all separation happens in the intended components.

Spent dilute is cooled until it precipitates. The excess salt is then added to the used concentrate, where it dissolves. Both electrolytes are now reset and may be fed back into the stack. This is illustrated in Fig. 2b.

To avoid high energy consumption for cooling, it is wise to choose a lower saturation temperature that corresponds to the temperature of any available cooling, e.g. seawater. The use of natural cooling will significantly reduce the energy consumption, and thus increase the potential for large scale operation.

Experimental

To investigate the membrane behaviour in the actual RED-system, the membranes are prepared in the relevant electrolytes and conductivities are measured at the relevant concentrations and temperatures.

Two membranes from Fumatech GmbH (Germany) were tested; FKE-50 (CEM) and FAS-30 (AEM) (see (7) and (5) for datasheets). The material datasheets for the membranes provide the conductivity of the membrane in NaCl form. Since this conductivity has been found through a different test procedure, we wanted to verify that our method gives similar results. The verification was successful and the results are given in Appendix A.

Membrane preparations

The ion-exchange is performed through soaking of the membranes in KNO_3 for more than 52 hours. KNO_3 of 1 M is used, and the solution is changed at least three times. The completeness of the exchange in the CEM is verified by measuring the pH of the spent solutions, comparing the value with fresh KNO_3 before immersion. It is considered satisfactory to soak the AEMs for more than three nights, well beyond what was needed for

the CEM, with solutions changed frequently. After soaking, the ion-exchanged membrane samples are prepared as round discs with a diameter of 20 mm, cut out with a wad punch.

In addition to the counter-ions that are present in the membrane due to the fixed charges, the membranes are believed to contain a small amount of solution with both anions and cations due to microcavities in the membrane structure (8). When the membranes are washed and soaked in deionized water (DI) after the KNO_3-equilibration, the co-ions, as well as the counter-ions superfluous to maintain electrical equilibrium, will be washed away. Conductivity measurements on these membranes are measuring the base conductivity of the membrane.

To compare and investigate how the membrane conductivity is impacted by electrolyte concentrations, the membranes are soaked in KNO_3 in addition to DI after the initial soaking and cutting. Batches of five samples are placed in individual vessels containing concentrations of 0 g/100g (DI), 10.1 g/100g (~1 M) and 25.3 g/100g (~2.5 M) aqueous KNO_3 for at least 24 hours. In addition, five samples are also placed in a vessel containing 45.6 g/100g (~4.5 M). This concentration equals the saturation temperature of KNO_3 at 30 °C.

Conductivity measurements

A series of measurements are performed to establish the membrane conductivity and its relation to concentration. The cell used to measure the conductivity is shown in Fig. 3. It consists of two electrodes with wire connectors, both made from platinum with a surface area of 3.14 cm^2 and a thickness of 1 mm. They are mounted in a hard cylindrical shell, with the connectors protruding from the ends. A sliding tube is fitted closely to the cylinder, providing structural integrity while sealing the cell and keeping the membrane samples immobile. This cylindrical cell shape is common when EIS is used for experiments of this kind (1, 16).
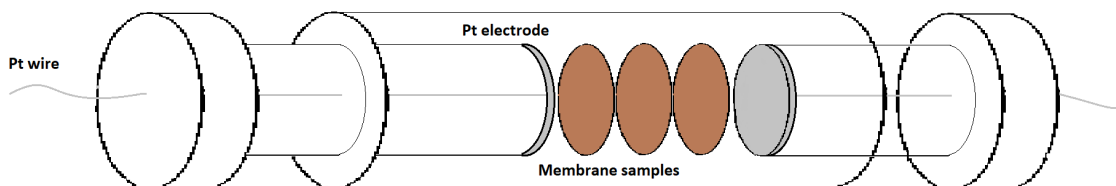

Figure 3. The cell used for measurements of conductivity

The membrane samples are placed between the electrodes of the conductivity cell. As the measurements are pressure sensitive, the cell is placed in a custom-made screw clamp, tightened with one bolt (M6, hexagonal head). A torque wrench is used to apply 2 Nm to the bolt, creating evenly distributed force due to the screw clamp. The electrodes of the conductivity cell are polished and fully polarised before use.

The conductivity experiments are performed at both 25 °C and 40 °C. In the latter case, both the cell and the samples are placed in a heating cabinet, long enough prior to

measurements to establish stationary temperature conditions. Temperature is measured by a K-type thermo-couple attached to the plastic shell directly behind, and in contact with, one of the platinum electrodes.

Measurements are performed with a Gamry Interface 5000E potentiostat, in a two-electrode setup. The experiments are performed through Hybrid EIS, with the potentiostat settings shown in Table I. Gamry Instruments Framework and Gamry Echem Analyst software are used to produce and analyse experimental data.

TABLE I. Hybrid EIS settings for the potentiostat

Variable	Value
AC voltage [mV rms]	**10**
DC voltage [mV rms]	**0**
Initial frequency [Hz]	**300 000**
Final frequency [Hz]	**1000**
Points/decade	**20**

Data extraction and obtaining of results

To account for inherent impedance from hardware, a blank experiment is run, where the electrodes are in contact. Eventually, the impedance spectrum for the dry cell at the relevant temperature is subtracted from all measurements prior to any further analysis.

The ohmic resistance, R [Ω], of the membranes is found as the high frequency resistance, where no capacitive effects are present in the measurements. In the impedance spectrum, this is the point where the imaginary part of the impedance is zero, manifesting as the intersect with the real axis. This intersection point is found through a linear regression of the impedance curve, in the range from 0 Ω to 4 Ω for the imaginary impedance.

The area resistance r [Ω m^2] is the measured resistance multiplied by the membrane sample area. r is plotted against the corresponding sample thickness. A linear regression is performed on each of the resulting plots, where the slope of each regression curve is the membrane resistivity, ρ [Ω m]. Every concentration yields one resistivity. The inverse of the resistivity is the membrane conductivity κ [S m^{-1}]. The conductivity values are then plotted against the concentrations, where the average of the four concentration-dependent conductivities is the reported membrane conductivity.

Modelling power density and hydrogen production

The unit cell power density is calculated from Eq. [4], with permselectivity and activity coefficients set to unity and a compartment thickness of 100 μm. The parameters are given in Table II in Appendix B. The resistances measured for the AEM and CEM are used in the calculation of the unit cell power density.

The power density is plotted versus current density, where the hydrogen production is calculated from the peak power current density and Faraday's law of electrolysis.

Results and Discussion

The conductivity, as function of concentration and temperature, are given in Fig. 4 and 5. The conductivity of K^+ in FKE-50 is found to be 4.5 ± 0.4 mS cm^{-1} at 25 °C and 6.6 ± 1.3 mS cm^{-1} at 40 °C. These values are higher than the reported values for Na^+ from Fuel Cell Store (6). The conductivity increase significantly from 25 °C to 40 °C, but the resistance of the membrane does not change considerably with concentration. This is in agreement with previous research (18).
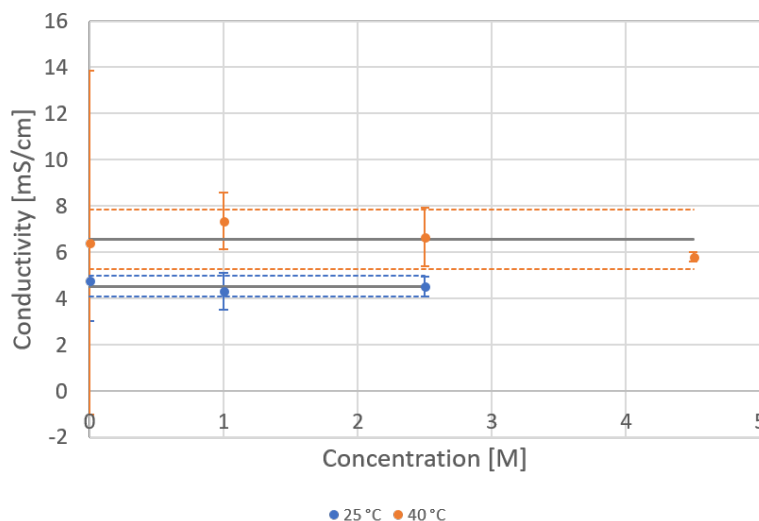
Figure 4. Conductivity of FKE-50 at 25 °C and 40 °C, with mean value and double standard deviation.

The conductivity of NO_3^- in FAS-30 was measured to 4.3 ± 1.2 mS cm^{-1} at 25 °C and 6.5 ± 2.3 mS cm^{-1} at 40 °C. These values are comparable to the reported values for Cl^- from Fuel Cell Store (5). The dependency of concentration is as negligible for FAS-30 as it is for FKE-50.

Given these resistances, the power density of one RED unit cell has been calculated and plotted versus current in Fig. 6. The maximum power density using 21.2 and 38.3 g KNO_3/ 100 g H_2O is 1.17 W m^{-2} at 25 °C and 1.38 W m^{-2} at 40 °C. For maximum solubility at 40 °C, 45.6 g KNO_3/ 100 g H_2O, the power density is 2.31 W m^{-2}.

Using solutions of 21.2 g and 38.3 g KNO_3/ 100 g H_2O, the hydrogen production at peak power is 2.97 and 3.27 g m^{-2} h^{-1} at 25 °C and 40 °C, respectively. When changing to 45.6 g KNO_3/ 100 g H_2O for the concentrated solution at 40 °C, the hydrogen production is 4.25 g m^{-2} h^{-1}.

If evaporation is to be used as separation technique, the dilute concentration can be lower. The maximum power density using 0.02 and 38.3 g KNO_3/ 100 g H_2O is 51.7 W m^{-2} at 25 °C and 101 W m^{-2} at 40 °C. Increasing the concentrated solution to maximum solubility at 40 °C, 45.6 g KNO_3, gives 108 W m^{-2} power density. Power density versus current density is shown in Fig. 7.
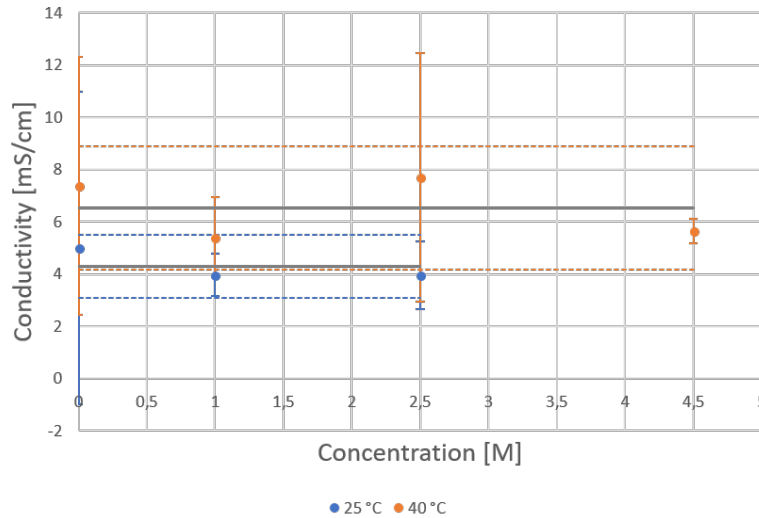
Figure 5. Conductivity of FAS-30 at 25 °C and 40 °C, with mean value and double standard deviation.
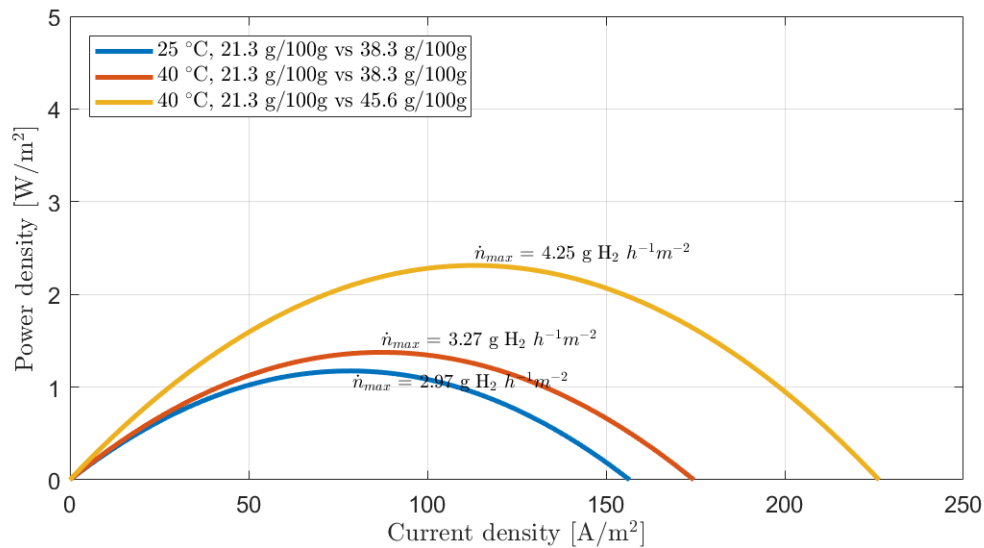

Figure 6. Power density from a RED unit cell. Concentrations are suited for use in the precipitation separation technique with KNO_3.

The hydrogen production at peak power is 14.4 and 26.9 g m^{-2} h^{-1} at 21.2 and 38.3 g KNO_3/ 100 g H_2O at 25 °C and 40 °C, respectively. At 45.6 g KNO_3 and 40 °C, the hydrogen production is 27.7 g m^{-2} h^{-1}.

The power density in the precipitation system is more dependent on concentration difference than change in temperature. For the evaporation system, however, the power density depends more on temperature then concentration difference.
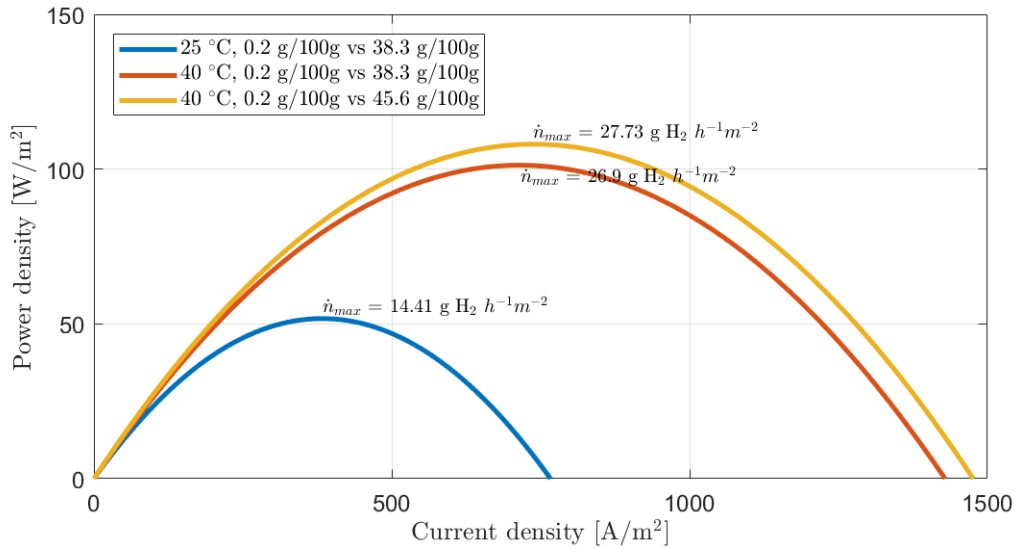
Figure 7. Power density from a RED unit cell. Concentrations are suited for use in the evaporation separation technique with KNO_3.

Conclusion

Two concepts for producing hydrogen from waste heat using RED were presented; one where salt is precipitated from spent dilute and one where water is evaporated from spent concentrate. As part of proof of concept for the precipitation method, the conductivity of a CEM and an AEM in KNO_3-form has been tested.

The results show that at 25 °C, FKE-50 has higher conductivity in K^+-form than in Na^+-form at 25 °C, while the average conductivity of FAS-30 in $NO3^-$-form is similar to its conductivity in Cl^--form. Neither of the membranes change conductivity with concentration of solution in the membrane.

The conductivity of K^+ in FKE-50 is significantly better at 40 °C than 25 °C. For FAS-30 the conductivity of NO_3^- is seemingly better at 40 °C than 25 °C, but the standard deviation is too high to confidently conclude. Based on these observations, KNO_3 is suitable for use in a RED system where solutions are regenerated by waste heat and higher conductivities are expected at 40 °C than 25 °C.

The peak power hydrogen production at maximum concentration difference is 4.25 g m^{-2} h^{-1} at 40 °C, and 2.97 g m^{-2} h^{-1} at 25 °C, for using precipitation. When using evaporation as separation technique, however, is the peak power hydrogen production 27.7 g m^{-2} h^{-1} at 40 °C and 14.4 g m^{-2} h^{-1} at 25 °C. The maximum peak power density available using evaporation is almost 50 times higher than the available maximum peak power density using precipitation. The precipitation as separation need to be equally less affordable to match the evaporation system.

References

1. E. Barsoukov and J. R. Macdonald. *Impedance spectroscopy: theory, experiment, and applications*. John Wiley & Sons, 2005.
2. O. S. Burheim. *Engineering Energy Storage*. Academic Press 2018, 2017.
3. P. Długołęcki, A. Gambier, K. Nijmeijer, and M. Wessling. *Environmental Science and Technology*, 43(17):6888–6894, 2009.
4. Enova SF. Annual Report 2009 - Enova. Technical report, Enova, 06 2010.
5. Fuel Cell Store. *Technical Data Sheet - fumasep®FAS-30*, 2018.
6. Fuel Cell Store. *Technical Data Sheet - fumasep®FKE-50*, 2018.
7. Fuel Cell Store. *Technical Data Sheet - fumasep®FKS-50*, 2018.
8. A. Galama, D. Vermaas, J. Veerman, M. Saakes, H. Rijnaarts, J. Post, and K. Nijmeijer. *Journal of Membrane Science*, 467:279 – 291, 2014.
9. E. Güler, R. Elizen, D. A. Vermaas, M. Saakes, and K. Nijmeijer. *Journal of Membrane Science*, 446:266 – 276, 2013.
10. M. C. Hatzell, I. Ivanov, R. D. Cusick, X. Zhu, and B. E. Logan. *Phys. Chem. Chem. Phys.*, 16:1632–1638, 2014.
11. T. Isono. *Journal of chemical and engineering data*, 29(1):45–52, 1984.
12. Y. Kim and B. E. Logan. *Proceedings of the National Academy of Sciences*, 108(39):16176–16181, 2011.
13. R. Lacey. *Ocean Engineering*, 7(1):1–47, 1980.
14. X. Luo, X. Cao, Y. Mo, K. Xiao, X. Zhang, P. Liang, and X. Huang. 19:25 – 28, 2012.
15. X. Luo, J.-Y. Nam, F. Zhang, X. Zhang, P. Liang, X. Huang, and B. E. Logan. *Bioresource Technology*, 140:399 – 405, 2013.
16. F. Müller, C. A. Ferreira, D. S. Azambuja, C. Alemán, and E. Armelin. *The Journal of Physical Chemistry B*, 118(4):1102–1112, 2014.
17. J.-Y. Nam, R. D. Cusick, Y. Kim, and B. E. Logan. *Environmental Science & Technology*, 46(9):5240–5246, 2012. PMID: 22463373.
18. J.-S. Park, J.-H. Choi, J.-J. Woo, and S.-H. Moon. 300(2):655 – 662, 2006.
19. R. Pattle. *Nature*, 174:660, 1954.
20. R. A. Tufa, E. Rugiero, D. Chanda, J. Hnàt, W. van Baak, J. Veerman, E. Fontananova, G. Di Profio, E. Drioli, K. Bouzek, et al. *Journal of Membrane Science*, 514:155–164, 2016.
21. W. J. van Egmond, U. K. Starke, M. Saakes, C. J. Buisman, and H. V. Hamelers. *Journal of Power Sources*, 340:71–79, 2017.
22. J. Weinstein and F. Leitz. *Science*, 191(4227):557–559, 1976. cited By 183.
23. G. L. Wick. *Energy*, 3(1):95–100, 1978.
24. X. Zhu, W. He, and B. E. Logan. *Journal of Membrane Science*, 494:154 – 160, 2015.

Appendix

A   Verification of conductivity measurement method

FKS-50 and FAS-30 are soaked in NaCl and tested the same way as the KNO_3-soaked membranes. The conductivity results are shown in Fig. 8 and 9.
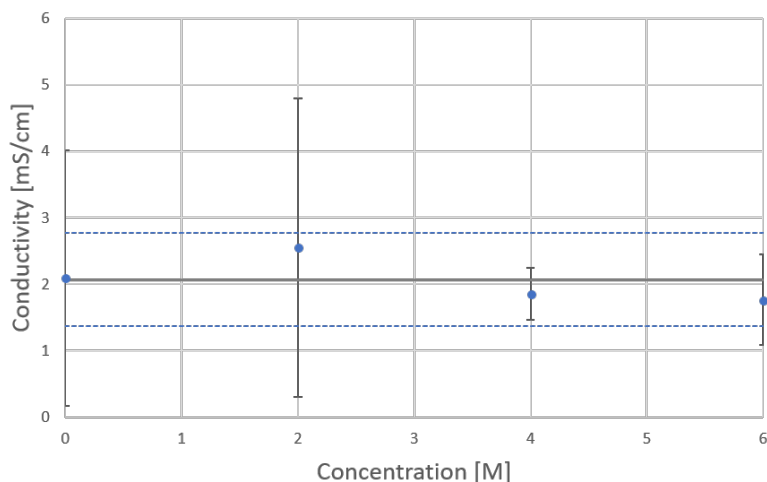

Figure 8. Conductivity of FKS-50 at 25 °C, with mean and double standard deviation.

The conductivity of Na^+ in FKS-50 was found to be 2.1 ± 0.7 mS cm^{-1} at 25 °C which is in the range of what Fuel Cell Store give in their datasheet for the given membrane (7).
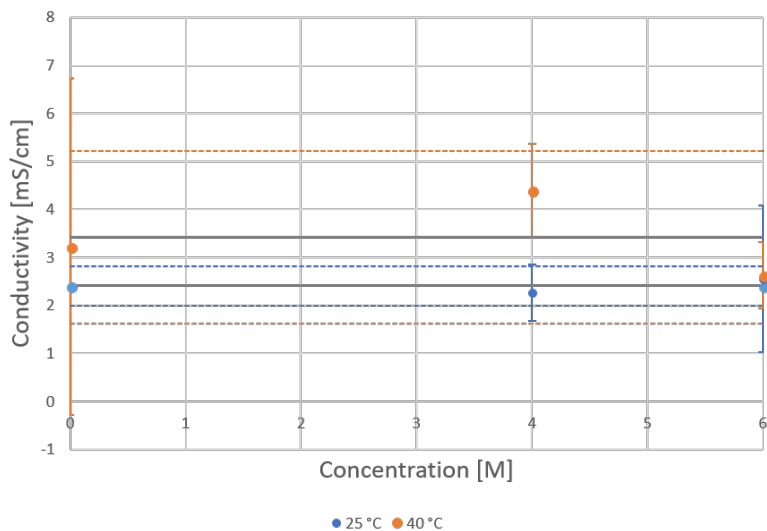

Figure 9. Conductivity of FAS-30 at 25 °C and 40 °C, with mean and double standard deviation. Fuel Cell Store reported 3-7 mS cm^{-1} at 25 °C.

The conductivity of of Cl^- in FAS-30 was found to be 2.4 ± 0.4 mS cm^{-1} and 3.4 ± 1.8 mS cm^{-1} at 25 °C and 40 °C respectively, which is within the lower range of what Fuel

Cell Store give in their datasheet for the given membrane. This means that our method does not overestimate the conductivity compared to the test provided in the datasheet.

B   Variable used in modelling cell potential and power density

TABLE II. Values used to calculate open circuit potential and unit cell resistance in RED

Variable name	Value
Mean permselectivity [-]	1
Temperature[K]	298 and 313
Activity coefficient [-]	1
Channel height [m]	1.00×10^{-4}
Resistivity 0.200 g KNO_3/100g H_2O 25 °C [Ω m^2]	1.67e-04**
Resistivity 0.200 g KNO_3/100g H_2O 40 °C [Ω m^2]	1.84e-06*
Resistivity 21.4 g KNO_3/100g H_2O 25 °C [Ω m^2]	6.83e-06**
Resistivity 21.4 g KNO_3/100g H_2O 40 °C [Ω m^2]	5.18e-08*
Resistivity 38.3 g KNO_3/100g H_2O 25 °C [Ω m^2]	5.12e-06**
Resistivity 38.3 g KNO_3/100g H_2O 40 °C [Ω m^2]	3.66e-08*
Resistivity 45.6 g KNO_3/100g H_2O 40 °C [Ω m^2]	3.46e-08*

*Measured for concentrations 0, 0.2, 2, 13.64, 21.36, 31.93 and 45.56 g / 100 g H_2O. Linear regression is used to find the resistance at the correct concentration.
**Found from (11). Linear regression is used to find the correct value.